2

A dual-input DC-DC converter using clean energy power supplies

Kei Eguchi
Shizuoka University
Japan

1. Introduction

For small color displays in portable devices, white LEDs have been used to provide one of the most ideal back-light solutions. To drive white LEDs in portable devices, switched-capacitor (SC) DC-DC converters (Bong (2009); Chung (2009); Doms (2009); Eguchi (2009a; 2010a;b); Gregoire (2006); Min (2002); Myono (2001); Park (2009); Starzyk (2001); Tanzawa (1997); Wei (2008); Yamada (2004); Yamakawa (2008)) have been used, because the capacitor-based converter can be designed without a magnetic element. Although the power efficiency of capacitor-based converters is inferior to that of inductor-based converters such as buck converters, boost converters, etc., inductor-less design enables capacitor-based converters to realize thin circuit composition, light-weight, no flux of magnetic induction, and so on.
In previous studies, single-input SC converters realizing step-up conversion (Chung (2009); Eguchi (2010b); Min (2002); Myono (2001); Park (2009); Starzyk (2001); Tanzawa (1997); Wei (2008)) have been used as a driver circuit of white LEDs. However, the single-input SC power converter is difficult to improve power efficiency by adjusting a voltage conversion ratio [1] , because the ratio of voltage conversion is predetermined by circuit structure. Therefore, the single-input SC converter is difficult to realize long battery runtime.
To solve this problem, multiple-input parallel converters (Eguchi (2009b); Ishikawa (2007); Kabe (2007); Qiu (2006)) using battery power supplies and clean energy power supplies have been proposed, where solar energy is usually used in mobile devices as a clean energy source. By converting solar energy, the multiple-input parallel converter can achieve long battery runtime. However, the hardware-cost of the parallel converter increases in proportion to the number of converter blocks although the parallel converter can be designed easily by connecting single SC DC-DC converters. Moreover, the parallel converter which consists of same converter blocks is difficult to achieve the wide range of clean energy inputs, because the ratio of the voltage conversion is predetermined by circuit structure although the value of input voltages from solar-cells changes depending on the weather conditions. To utilize solar energy for back-lighting applications effectively, the SC DC-DC converter which can realize not only small hardware-cost but also wide input-range is required.
In this chapter, a switched-capacitor-based serial DC-DC converter is proposed. The converter consists of 2 converter blocks, where the Block-1 is the step-up/step-down SC DC-DC

[1] To adjust the output voltage, pulse width modulation (PWM) scheme or on-resistance control scheme is usually employed in the SC DC-DC converter.

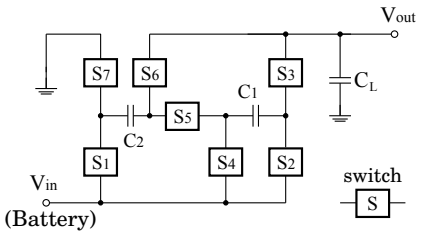

Fig. 1. Conventional single-input converter

Ratio	Phase	On	Off
2×	Charging	S_3, S_4, S_5, S_7	S_1, S_2, S_6
	Transfer	S_1, S_3, S_4, S_6	S_2, S_5, S_7
1.5×	Charging	S_2, S_5, S_7	S_1, S_3, S_4, S_6
	Transfer	S_1, S_3, S_4, S_6	S_2, S_5, S_7

Table 1. Setting of clock pulses

converter using battery energy and the Block-2 is a quasi-switched-capacitor cell (Pan (2007)) using solar energy. The hardware-cost of the quasi-SC cell (Pan (2007)) is much smaller than that of the conventional single-input converter (Chung (2009); Eguchi (2010b); Min (2002); Myono (2001); Park (2009); Starzyk (2001); Tanzawa (1997); Wei (2008)). Therefore, the proposed converter can realize small hardware-cost. Furthermore, unlike conventional SC DC-DC converters, the output voltage of the proposed converter is generated by adding the output voltage of the SC-based circuit to the voltage of solar-cells. In the Block-1, the voltage conversion ratio is controlled according to the variation of the voltage of solar cells. Therefore, the proposed converter can realize wide input-range.
Concerning the proposed serial converter, theoretical analyses and SPICE simulations are performed to investigate the circuit characteristics. Furthermore, to confirm the validity of circuit design, experiments are performed concerning the experimental circuit fabricated with commercially available transistors on a bread board.

2. Circuit Structure

2.1 Single-Input Converter

Figure 1 shows an example of the single-input converter. The converter of figure 1 is one of the most famous converters and is adopted for MAX1910, MAX1912 [2] , and so on. According to the control rule shown in Table 1, power switches $S_1 \sim S_7$ in figure 1 are driven by 2-phase clock pulses, synchronously. By controlling $S_1 \sim S_7$, the conventional converter shown in figure 1 generates $1.5 \times /2\times$ stepped-up voltages. However, as Table 1 shows, the single-input converter is difficult to improve power efficiency further by adjusting a voltage conversion

[2] MAX1910 and MAX1912 are $1.5 \times /2\times$ step-up converters produced by Maxim Integrated Products. In mobile back-lighting applications, the stepped-up voltage such as $4.75 \sim 6.5$ V (Typ. =5 V) is required to drive some LEDs from the voltage of a lithium battery. The typical voltage of the lithium battery used in the mobile equipments is about 3.7 V.

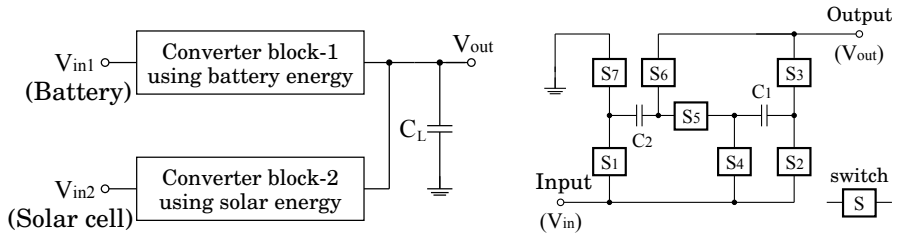

(a) Block diagram (b) Converter block

Fig. 2. Conventional multiple-input parallel converter

ratio, because the ratio of the voltage conversion is predetermined by circuit structure. Therefore, since the single-input converter only consumes energy stored in the battery, it is difficult for the single-input converter to realize long battery runtime.

2.2 Parallel-Connected Converter

To realize long battery runtime, the multiple-input converter has been proposed (Ishikawa (2007); Kabe (2007); Qiu (2006)). As described in (Ishikawa (2007); Kabe (2007); Qiu (2006)), the multiple-input converter can be designed easily by connecting single-input DC-DC converters in parallel.

Figure 2 shows an example of the multiple-input parallel converter designed by using switched-capacitor (SC) techniques, where battery energy and solar energy are used as input energy sources. The multiple-input converter can realize long battery runtime, because the consumption of battery energy is suppressed by converting solar energy. However, the hardware-cost of the parallel converter increases in proportion to the number of converter blocks. Furthermore, the parallel converter which consists of same converter blocks is difficult to realize the wide range [3] of clean energy inputs, because the ratio of the voltage conversion is predetermined by the circuit structure of converter blocks although the voltage of solar-cells changes depending on the weather conditions.

Of course, the parallel converters can achieve the wide input range by connecting different kinds of converters according to input sources. However, although the wide input range is realized by using different kinds of converters, the problem of hardware-cost cannot be solved. To make matters worse, this approach not only causes the complexity of circuit control but also ruins the simplicity of circuitry. To utilize solar energy effectively, the SC DC-DC converter which can realize not only small hardware-cost but also wide input-range is required.

2.3 Proposed Converter

Figure 3 shows the proposed serial DC-DC converter. The converter consists of 2 converter blocks, where the Block-1 is the step-up/step-down SC DC-DC converter using battery energy and the Block-2 is a switched-capacitor-based converter using solar energy. Unlike conventional converters, the output voltage of the proposed converter is generated by adding the

[3] Only when $V_{in2} \geq V_{tag}/2$, the conventional converter of figure 2 can offer the stepped-up voltage V_{tag} to drive some LEDs from clean energy power supplies. Concretely, the voltage from solar-cells, V_{in2}, must be more than 2.5 V when target output voltage V_{tag} is 5 V.

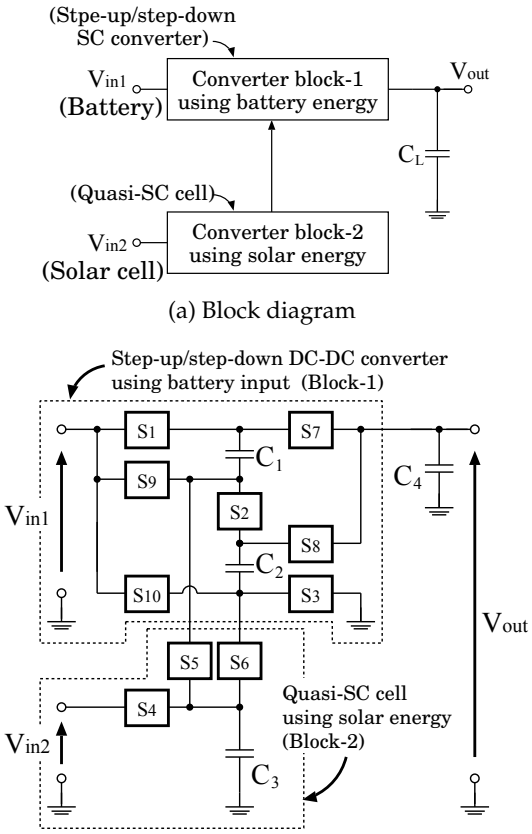

Fig. 3. Proposed dual-input serial converter

output voltage of an SC-based circuit to the voltage of solar-cells. According to the voltage of solar-cells, the proposed converter changes the operation modes as shown in Table 2, where V_{tag} (Typ. =5 V) denotes the target output voltage ($\simeq 3V_{in1}/2$) to drive LEDs.
To realize the operation modes shown in Table 2, power switches $S_1 \sim S_{10}$ in figure 3 are driven by 2-phase clock pulses, synchronously. By controlling $S_1 \sim S_{10}$, the proposed converter performs a step-up DC-DC conversion. Table 3 shows the setting of clock pulses. In Table 3, the interval of $Charging$ $(= State - T1)$ and $Transfer$ $(= State - T2)$ is set to

$$\begin{aligned} & T = T1 + T2, \\ & T1 = DT, \\ \text{and} \quad & T2 = (1 - D)T, \end{aligned} \tag{1}$$

where D and T denote the duty factor and the period of the clock pulses, respectively.

	Input voltage V_{in2}	Conversion ration	
		Block-1	Block-2
Mode-1	$\frac{2V_{tag}}{3} \leq V_{in2}$	$\frac{1}{2}\times$	$1\times$
Mode-2	$\frac{V_{tag}}{3} \leq V_{in2} < \frac{2V_{tag}}{3}$	$1\times$	$1\times$
Mode-3	$V_{in2} < \frac{V_{tag}}{3}$	$\frac{3}{2}\times$	$0\times$

Table 2. Setting of conversion ratio

	Phase	On	Off
Mode-1	Charging $(State-T1)$	S_1, S_2, S_3, S_4	$S_5, S_6, S_7, S_8, S_9, S_{10}$
	Transfer $(State-T2)$	S_5, S_6, S_7, S_8	$S_1, S_2, S_3, S_4, S_9, S_{10}$
Mode-2	Charging $(State-T1)$	S_1, S_2, S_3, S_4	$S_5, S_6, S_7, S_8, S_9, S_{10}$
	Transfer $(State-T2)$	S_2, S_6, S_7	$S_1, S_3, S_4, S_5, S_8, S_9, S_{10}$
Mode-3	Charging $(State-T1)$	S_1, S_2, S_3	$S_4, S_5, S_6, S_7, S_8, S_9, S_{10}$
	Transfer $(State-T2)$	S_7, S_8, S_9, S_{10}	$S_1, S_2, S_3, S_4, S_5, S_6$

Table 3. Setting of clock pulses

Figure 4 shows the comparison concerning the input range of figures 2 and 3. As figure 4 shows, the proposed converter can extend the input range of V_{in2} from $V_{in2} \geq V_{tag}/2$ to $V_{in2} \geq V_{tag}/3$. Concretely, in comparison with the conventional parallel converter using $1.5\times$ step-up converters, the proposed converter can achieve 16% extension of input range.
Furthermore, the proposed converter can realize small hardware-cost. Table 4 shows the comparison concerning the hardware-cost of figures 2 and 3. As Table 4 shows, the hardware-cost of the proposed converter is less than 80 % of that of the conventional converter.
The circuit properties of the proposed serial converter will be described in the following section.

3. Theoretical Analysis

First, the equivalent circuit of the proposed converter is analyzed. To save space, only the analysis for Mode-1 is described in this section [4] . In the theoretical analysis, we assume that 1. parasitic elements are negligibly small and 2. time constant is much larger than the period of clock pulses.
Figure 5 shows instantaneous equivalent circuits of the proposed converter. In figure 5, R_{on} [5] denotes the on-resistance of power switches.

[4] The theoretical analysis for Mode-2 and Mode-3 will be described in Appendix.
[5] SC power converters are known as an implementable converter, because they do not require magnetic elements. In the converter block implemented into a chip, the direction of fluctuation in on-resistances is almost the same. Therefore, to simplify the theoretical analysis, we assume that all the power switches have the same on-resistances.

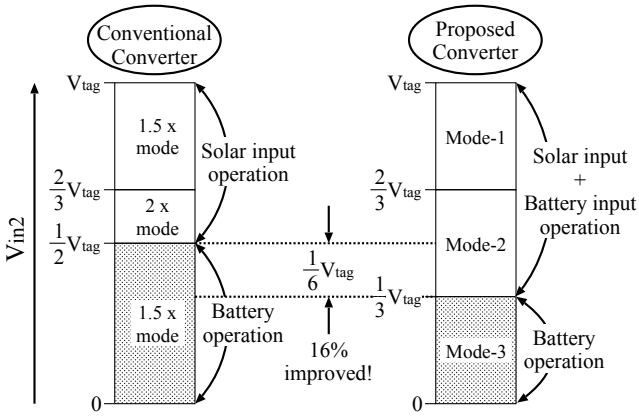

Fig. 4. Comparison concerning input range of V_{in2}

	Number of switches	Number of capacitors
Conventional converter	14	5
Proposed converter	10 (71 %)	4 (80 %)

Table 4. Comparison concerning hardware cost

In the steady state of figure 5, differential values of the electric charges in C_k $(k = \{1, 2, 3, 4\})$ satisfy

$$\Delta q_{T1}^k + \Delta q_{T2}^k = 0, \tag{2}$$

where Δq_{T1}^k and Δq_{T2}^k denote electric charges when $State - T1$ and $State - T2$, respectively. In the case of $State - T1$, differential values of the electric charges in the input and the output terminals, $\Delta q_{T1,V_{in1}}$, $\Delta q_{T1,V_{in2}}$, and $\Delta q_{T1,V_{out}}$, are given by

$$\begin{aligned} &\Delta q_{T1,V_{in1}} = \Delta q_{T1}^1 = \Delta q_{T1}^2, \\ &\Delta q_{T1,V_{in2}} = \Delta q_{T1}^3, \\ \text{and} \quad &\Delta q_{T1,V_{out}} = \Delta q_{T1}^4. \end{aligned} \tag{3}$$

On the other hand, in the case of $State - T2$, differential values of the electric charges in the input and the output terminals, $\Delta q_{T2,V_{in1}}$, $\Delta q_{T2,V_{in2}}$, and $\Delta q_{T2,V_{out}}$, are given by

$$\begin{aligned} &\Delta q_{T2,V_{in1}} = 0, \\ &\Delta q_{T2,V_{in2}} = 0, \\ \text{and} \quad &\Delta q_{T2,V_{out}} = \Delta q_{T2}^1 + \Delta q_{T2}^2 + \Delta q_{T2}^4. \end{aligned} \tag{4}$$

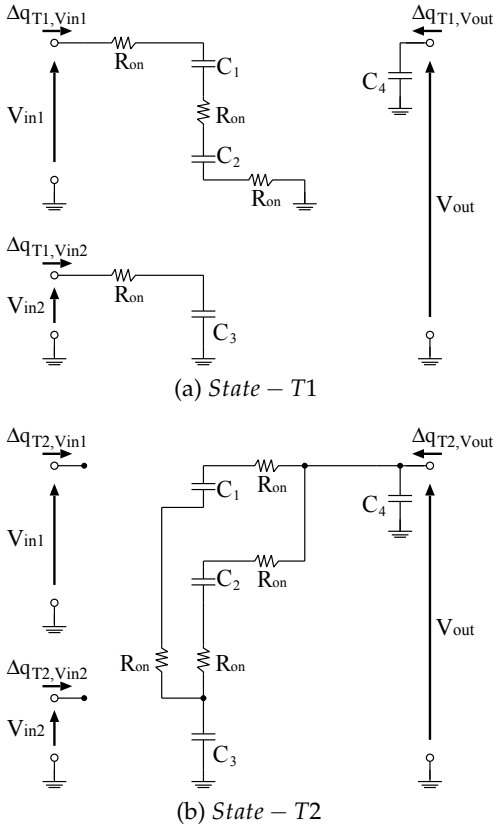

Fig. 5. Instantaneous equivalent circuits when $2V_{tag}/3 \leq V_{in2}$

Furthermore, in figure 5, the following condition is satisfied:

$$\Delta q^3_{T2} = \Delta q^1_{T2} + \Delta q^2_{T2}. \tag{5}$$

Here, average currents of the inputs and the output are given by

$$\begin{aligned} \overline{I_{in1}} &= (\Delta q_{T1,V_{in1}} + \Delta q_{T2,V_{in1}})/T \\ &\equiv \Delta q_{V_{in1}}/T, \\ \overline{I_{in2}} &= (\Delta q_{T1,V_{in2}} + \Delta q_{T2,V_{in2}})/T \\ &\equiv \Delta q_{V_{in2}}/T, \\ \text{and} \quad \overline{I_{out}} &= (\Delta q_{T1,V_{out}} + \Delta q_{T2,V_{out}})/T \\ &\equiv \Delta q_{V_{out}}/T, \end{aligned} \tag{6}$$

where $\Delta q_{V_{in1}}$, $\Delta q_{V_{in2}}$, and $\Delta q_{V_{out}}$ are electric charges in the input terminal-1, the input terminal-2, and the output terminal, respectively. From equations (2) $\sim$ (6), the relation between the

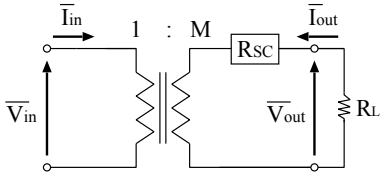

Fig. 6. General form of equivalent circuit

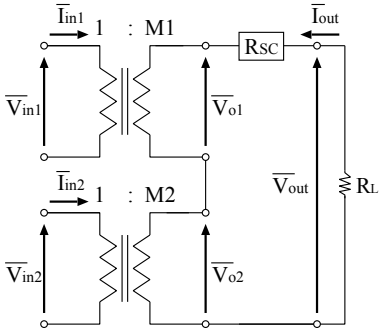

Fig. 7. Equivalent circuit of proposed converter

input currents and the output current are derived:

$$\overline{I_{in1}} = -\frac{1}{2}\overline{I_{out}}$$
$$\text{and} \qquad \overline{I_{in2}} = -\overline{I_{out}}. \tag{7}$$

In figure 5, the energy consumed by resistors in one period, W_T, can be expressed as

$$W_T \quad = \quad W_{T1} + W_{T2}, \tag{8}$$

where

$$W_{T1} = \frac{3R_{on}}{T1}(\Delta q_{T1}^1)^2 + \frac{R_{on}}{T1}(\Delta q_{T1}^3)^2 \tag{9}$$
$$\text{and} \qquad W_{T2} = \frac{2R_{on}}{T2}(\Delta q_{T2}^1)^2 + \frac{2R_{on}}{T2}(\Delta q_{T2}^2)^2. \tag{10}$$

From equations (2) $\sim$ (7), equations (9) and (10) can be rewritten as

$$W_{T1} = \frac{7R_{on}}{4DT}(\Delta q_{V_{out}})^2 \tag{11}$$
$$\text{and} \qquad W_{T2} = \frac{R_{on}}{(1-D)T}(\Delta q_{V_{out}})^2. \tag{12}$$

Input voltage V_{in2}	R_{SC}	$M1$	$M2$
$\frac{2V_{tag}}{3} \leq V_{in2}$	$\frac{(7-3D)R_{on}}{4D(1-D)}$	$\frac{1}{2}$	1
$\frac{V_{tag}}{3} \leq V_{in2} < \frac{2V_{tag}}{3}$	$\frac{(4-D)R_{on}}{D(1-D)}$	1	1
$V_{in2} < \frac{V_{tag}}{3}$	$\frac{(3+D)R_{on}}{4D(1-D)}$	$\frac{3}{2}$	0

Table 5. Theoretical results of other conversion ratios

Here, a general equivalent circuit of SC power converters (Eguchi (2009a;b; 2010a;b)) can be given by the circuit shown in figure 6, where R_{SC} is called the SC resistance, M is the ratio of an ideal transformer, and $\overline{V_{in}}$ and $\overline{V_{out}}$ denote the averaged input voltage and the averaged output voltage, respectively. The consumed energy W_T in figure 6 can be defined by

$$\begin{aligned} W_T &= W_{T1} + W_{T2} \\ &\equiv (\frac{\Delta q_{V_{out}}}{T})^2 \cdot R_{SC} \cdot T. \end{aligned} \tag{13}$$

By substituting equations (11) and (12) into equation (13), SC resistance R_{SC} for Mode-1 is given by

$$R_{SC} = \frac{7-3D}{4D(1-D)} \cdot R_{on}. \tag{14}$$

The equivalent circuit shown in figure 6 can be expressed by the determinant using the Kettenmatrix. Therefore, by using equations (7) and (14), the equivalent circuit of the proposed step-up converter can be given by the circuit shown in figure 7 and the following determinants:

$$\begin{bmatrix} \overline{V_{in1}} \\ \overline{I_{in1}} \end{bmatrix} = \begin{bmatrix} 1/M1 & 0 \\ 0 & M1 \end{bmatrix} \begin{bmatrix} \overline{V_{o1}} \\ \overline{I_{out}} \end{bmatrix}, \tag{15}$$

$$\begin{bmatrix} \overline{V_{in2}} \\ \overline{I_{in2}} \end{bmatrix} = \begin{bmatrix} 1/M2 & 0 \\ 0 & M2 \end{bmatrix} \begin{bmatrix} \overline{V_{o2}} \\ \overline{I_{out}} \end{bmatrix}, \tag{16}$$

$$\begin{bmatrix} \overline{V_{o1}} + \overline{V_{o2}} \\ \overline{I_{out}} \end{bmatrix} = \begin{bmatrix} 1 & R_{SC} \\ 0 & 1 \end{bmatrix} \begin{bmatrix} \overline{V_{out}} \\ -\overline{I_{out}} \end{bmatrix}, \tag{17}$$

where $M1 = 1/2$ and $M2 = 1$. To save space, only the conversion mode in the case of $2V_{tag}/3 \leq V_{in2}$ was discussed in this section. However, other cases can also be analyzed by the same method. Table 5 shows parameters $M1$, $M2$, and R_{SC} of other modes.
By using equations (15) $\sim$ (17) and figure 7, power efficiency η [6] can be expressed by

$$\begin{aligned} \eta &= \frac{R_L(\overline{I_{out}})^2}{R_L(\overline{I_{out}})^2 + R_{SC}(\overline{I_{out}})^2} \\ &= \frac{R_L}{R_L + R_{SC}}, \end{aligned} \tag{18}$$

[6] Of course, the consumed energy of peripheral circuits such as pulse generators, comparators, etc. is disregarded in the power efficiency of equation (18).

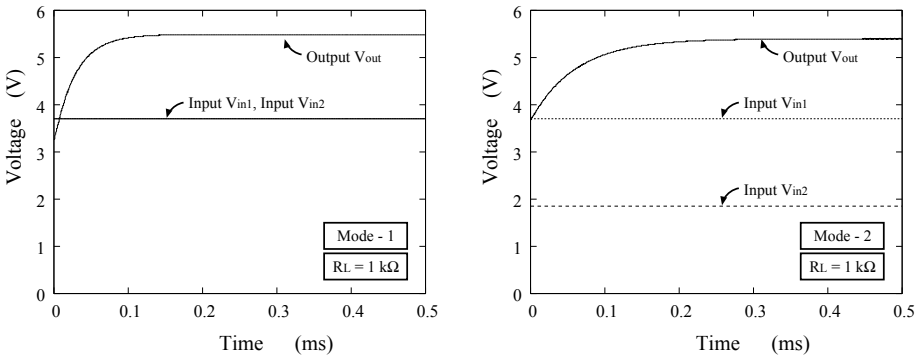

(a) Mode-1 (b) Mode-2

Fig. 8. Output voltage of proposed converter

where the optimal value of parameter D is obtained when

$$\frac{dR_{SC}}{dD} = 0 \quad \text{and} \quad 0 < D < 1. \tag{19}$$

Concretely, from equations (14) and (19), the optimal duty factor is $D \simeq 0.57$ for Mode-1.

4. Simulation

To confirm the validity of the theoretical analysis, SPICE simulations were performed under conditions where where V_{in1} = 3.7 V, $C_1 \sim C_4$ = 2 μF, $T = 1\,\mu s$, $D = 0.5$, and $R_{on} = 2$ ohm.
Figure 8 shows the output voltage of the proposed converter, where the output voltage was not regulated. In figure 8, input voltage V_{in2} for Mode-1 and Mode-2 was set to $V_{in2} = V_{in1}$ and $V_{in2} = V_{in1}/2$, respectively. As figure 8 shows, in spite of the change in V_{in2}, the proposed converter can generate the stepped-up output voltage. In other words, the proposed converter can realize wide input-range of V_{in2}.
Figure 9 shows the power efficiency of the proposed converter as a function of output load R_L. In figure 9, input voltage V_{in2} for Mode-1 and Mode-2 was set to $V_{in2} = V_{in1}$ and $V_{in2} = V_{in1}/2$, respectively. As figure 9 shows, theoretical results correspond well with simulated results. For this reason, the derived theoretical formulas will be helpful to design the series converter. Of course, the power efficiency can be improved by using power-switches with small on-resistance.

5. Experiment

To confirm the validity of circuit design, experiments were performed regarding to the proposed converter shown in figure 3. The experimental circuit was built with commercially available transistors on a bread board.
Figures 10, 11, and 12 show the experimental results of the bread board circuit, where input voltages capacitors V_{in1} = 3.7 V, $C_1 \sim C_4 = 3.3\mu$F, $R_L = 10$kohm, $T = 100\mu$s, and $D = 0.5$. In figures 10, 11, and 12, input voltage V_{in2} was set to about 3.7 V, 1.8 V, and 0 V, respectively.

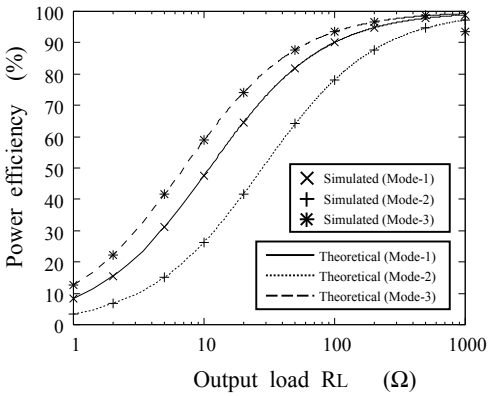

Fig. 9. Power efficiency as function of output load R_L

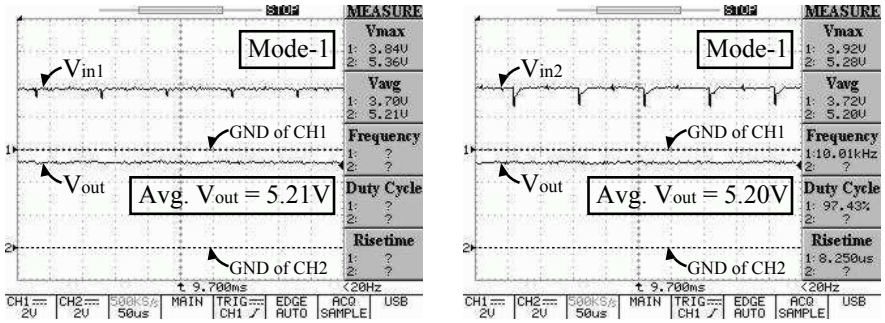

(a) V_{out} vs. V_{in1} (b) V_{out} vs. V_{in2}

Fig. 10. Measured output voltages for Mode-1

As these figures show, the circuit design of the proposed converter is appropriate, because the stepped-up voltage about 5 V can be generated [7] .

6. Conclusion

In this chapter, a serial SC DC-DC converter using clean energy power supplies has been proposed.

The validity of the circuit design was confirmed by theoretical analyses, SPICE simulations, and experiments. The proposed converter can realize not only long battery runtime but also small hardware-cost and wide input-range. Concretely, in comparison with the conventional parallel converter using 1.5× step-up SC converters, the proposed converter can achieve 20%

[7] In the experiment, the circuit properties such as power efficiency, ripple noise, etc. were not examined, because the experimental circuit was built with commercially available transistors on the bread board. Only the circuit design was verified through the experiments, because the parasitic resistance of the bread board is very large unlike an IC chip.

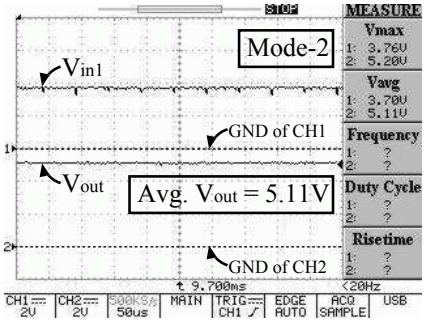

(a) V_{out} vs. V_{in1}

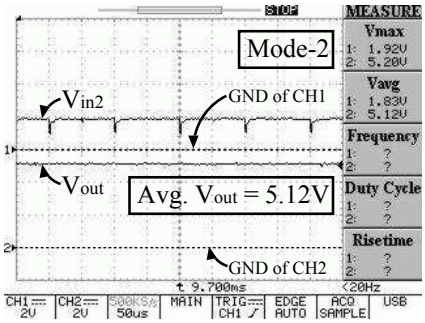

(b) V_{out} vs. V_{in2}

Fig. 11. Measured output voltages for Mode-2

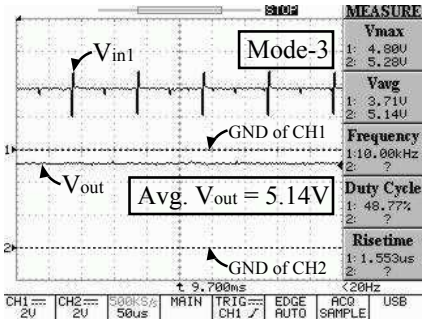

(a) V_{out} vs. V_{in1}

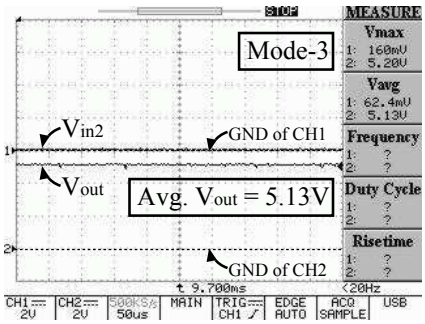

(b) V_{out} vs. V_{in2}

Fig. 12. Measured output voltages for Mode-3

reduction of hardware cost and 16% extension of input range. Furthermore, the derived theoretical formulas can provide basic information to design serial SC DC-DC converters, because theoretical results corresponded well with SPICE simulation results. The proposed converter will be useful as a driver circuit of white LEDs for display back-lighting.
The IC implementation and experiments are left to a future study.

Appendix

Theoretical analysis for Mode-2

In this section, the characteristics of the proposed converter for $V_{tag}/3 \leq V_{in2} < 2V_{tag}/3$ is analyzed theoretically. The conditions of this theoretical analysis are the same as that shown in section 3.
Figure 13 shows the instantaneous equivalent circuits for Mode-2. In the steady state, the differential value of electric charges in C_k $(k = \{1,2,3,4\})$ satisfies equation (2). In the case of $State - T1$, differential values of electric charges in the input terminals and the output

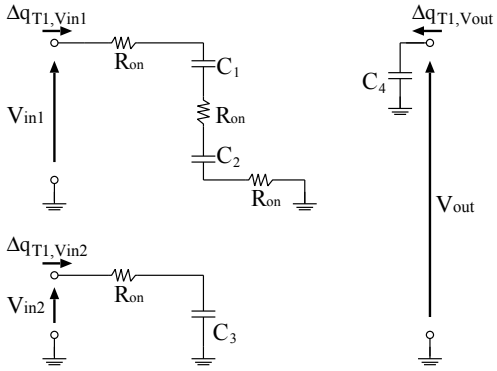

(a) $State - T1$

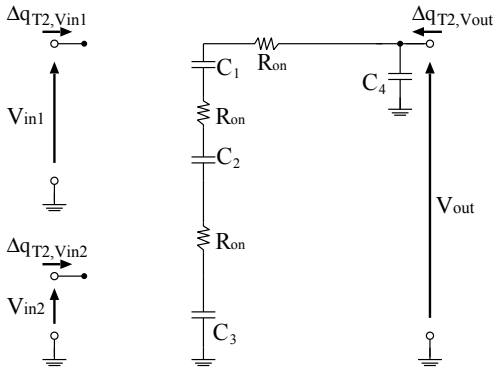

(b) $State - T2$

Fig. 13. Instantaneous equivalent circuits when $V_{tag}/3 \leq V_{in2} < 2V_{tag}/3$

terminal, $\Delta q_{T1,V_{in1}}$, $\Delta q_{T1,V_{in2}}$, and $\Delta q_{T1,V_{out}}$, are given by

$$\begin{aligned} \Delta q_{T1,V_{in1}} &= \Delta q^1_{T1} - \Delta q^2_{T1}, \\ \Delta q_{T1,V_{in2}} &= \Delta q^3_{T1}, \\ \text{and} \quad \Delta q_{T1,V_{out}} &= \Delta q^4_{T1}. \end{aligned} \tag{20}$$

In the case of $State - T2$, differential values of electric charges in the input terminals and the output terminal, $\Delta q_{T2,V_{in1}}$, $\Delta q_{T2,V_{in2}}$, and $\Delta q_{T2,V_{out}}$, are given by

$$\begin{aligned} \Delta q_{T2,V_{in1}} &= 0, \\ \Delta q_{T2,V_{in2}} &= 0, \\ \text{and} \quad \Delta q_{T2,V_{out}} &= \Delta q^1_{T2} + \Delta q^4_{T2} = \Delta q^2_{T2} + \Delta q^4_{T2} = \Delta q^3_{T2} + \Delta q^4_{T2}. \end{aligned} \tag{21}$$

By substituting equations (2), (20), and (21) into equation (6), the following equations are derived:

$$\overline{I_{in1}} = -\overline{I_{out}} \quad \text{and} \quad \overline{I_{in2}} = -\overline{I_{out}}. \tag{22}$$

In figure 13, the energy consumed by resistors in one period, W_T, can be expressed as

$$W_T = W_{T1} + W_{T2}, \tag{23}$$

where

$$W_{T1} = \frac{3R_{on}}{T_1}(\Delta q_{T1}^1)^2 + \frac{R_{on}}{T_1}(\Delta q_{T1}^3)^2$$
$$\text{and} \qquad W_{T2} = \frac{3R_{on}}{T_2}(\Delta q_{T2}^1)^2.$$

From equations (2), (20), and (21), equation (23) can be rewritten as

$$W_T = \frac{4R_{on}}{DT}(\Delta q_{V_{out}})^2 + \frac{3R_{on}}{(1-D)T}(\Delta q_{V_{out}})^2. \tag{24}$$

Thus, from equations (13) and (24), the SC resistance R_{SC} is given by

$$R_{SC} = \frac{(4-D)R_{on}}{D(1-D)}. \tag{25}$$

Therefore, by using equations (22) and (25), the equivalent circuit can be expressed by the circuit shown in figure 7 and equations (15) $\sim$ (17), where $M1 = 1$ and $M2 = 1$. The power efficiency can also be obtained by equation (18), where the optimal duty factor is $D \simeq 0.67$ when $V_{tag}/3 \leq V_{in2} < 2V_{tag}/3$.

Theoretical analysis for Mode-3

Next, the characteristics of the proposed converter for $2V_{tag}/3 \leq V_{in2}$ is analyzed theoretically. Figure 14 shows the instantaneous equivalent circuits when Mode-3. In the steady state, the differential value of electric charges in C_k ($k = \{1, 2, 3, 4\}$) satisfies equation (2). In the case of $State - T1$, $\Delta q_{T1,V_{in1}}$, $\Delta q_{T1,V_{in2}}$, and $\Delta q_{T1,V_{out}}$, are given by

$$\Delta q_{T1,V_{in1}} = \Delta q_{T1}^1 = \Delta q_{T1}^2,$$
$$\Delta q_{T1,V_{in2}} = 0,$$
$$\text{and} \qquad \Delta q_{T1,V_{out}} = \Delta q_{T1}^4. \tag{26}$$

On the other hand, in the case of $State - T2$, $\Delta q_{T2,V_{in1}}$, $\Delta q_{T2,V_{in2}}$, and $\Delta q_{T2,V_{out}}$, are given by

$$\Delta q_{T2,V_{in1}} = -\Delta q_{T1}^2 - \Delta q_{T2}^2,$$
$$\Delta q_{T2,V_{in2}} = 0,$$
$$\text{and} \qquad \Delta q_{T2,V_{out}} = \Delta q_{T2}^1 + \Delta q_{T2}^2 + \Delta q_{T2}^4. \tag{27}$$

By substituting equations (2), (26), and (27) into equation (6), the following equation is derived:

$$\overline{I_{in1}} = -\frac{3}{2}\overline{I_{out}} \quad \text{and} \quad \overline{I_{in2}} = 0. \tag{28}$$

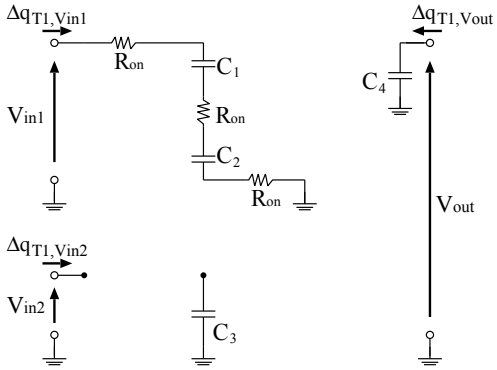

(a) $State - T1$

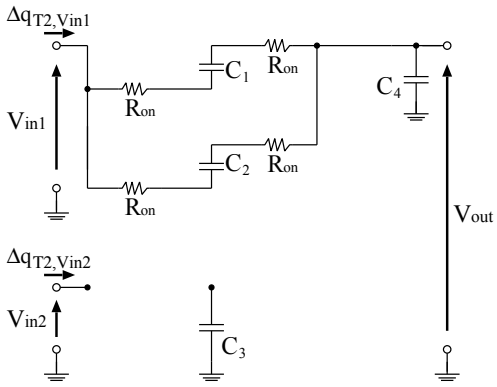

(b) $State - T2$

Fig. 14. Instantaneous equivalent circuits when $2V_{tag}/3 \leq V_{in2}$

In figure 14, the energy consumed by resistors in one period, W_T, can be expressed as

$$W_T = W_{T1} + W_{T2}, \tag{29}$$

where

$$W_{T1} = \frac{3R_{on}}{T_1}(\Delta q_{T1}^1)^2$$

and $$W_{T2} = \frac{2R_{on}}{T_2}(\Delta q_{T2}^1)^2 + \frac{2R_{on}}{T_2}(\Delta q_{T2}^2)^2.$$

From equations (2), (26), and (27), equation (29) can be rewritten as

$$W_T = \frac{3R_{on}}{4DT}(\Delta q_{V_{out}})^2 + \frac{R_{on}}{(1-D)T}(\Delta q_{V_{out}})^2. \tag{30}$$

Thus, from equations (13) and (30), the SC resistance R_{SC} is given by

$$R_{SC} = \frac{(3+D)R_{on}}{4D(1-D)}. \tag{31}$$

Therefore, by using equations (28) and (31), the equivalent circuit can be expressed by the circuit shown in figure 7 and equations (15) $\sim$ (17), where $M1 = 3/2$ and $M2 = 0$. The power efficiency can also be obtained by equation (18), where the optimal duty factor is $D \simeq 0.46$ when $2V_{tag}/3 \leq V_{in2}$.

7. References

Bong, J.H.; Kwon, Y.J.; Kim, D. & Min,K.S. (2009). Negative charge pump circuit with large output current and high power efficiency. *IEICE Electronics EXpress*, Vol.6 (No.6): 304-309. ISSN 1349-2543

Chung, I.Y. & Shin, J. (2009). New charge pump circuits for high output voltage and large current drivability. *IEICE Electronics EXpress*, Vol.6 (No.12): 800-805. ISSN 1349-2543

Doms, I.; Merken, P.; Hoof, C.V. & Mertens, R.P. (2009). Capacitive power management circuit for micropower thermoelectric generators with a 1.4μA controller. *IEEE, J. Solid-State Circuits*, Vol.44 (No.10): 2824-2833. ISSN 0018-9200

Eguchi, K.; Oota, I.; Terada, S. & Inoue, T. (2009). A design method of switched-capacitor power converters by employing a ring-type power converter. *Int. J. of Innovative Computing, Information and Control*, Vol.5 (No.10 (A)): 2927-2938. ISSN 1349-4198

Eguchi, K.; Pongswatd, S.; Tirasesth, K. & Sasaki, H. (2009). Synthesis and analysis of a multiple-input parallel SC DC-DC converter. *Proceedings of the 2009 ECTI International Conference*, pp.306-309, ISBN 978-1-4244-3388-9, Thailand, May 2009, the Institute of Electrical and Electronics Engineers, Piscataway

Eguchi, K.; Pongswatd, S.; Tirasesth, K.; Sasaki, H. & Inoue, T. (2010). Optimal design of a single-input parallel DC-DC converter designed by switched capacitor techniques. *Int. J. of Innovative Computing, Information and Control*, Vol.6 (No.1 (A)): 215-227. ISSN 1349-4198

Eguchi, K.; Pongswatd, S.; Julsereewong, A.; Tirasesth, K.; Sasaki, H. & Inoue, T. (2010). Design of a multiple-input SC DC-DC converter realizing long battery runtime. *IEICE, Fundamentals*, Vol.E93-A (No.5): 985-988. ISSN 1745-1337

Gregoire, B.R. (2006). A compact switched-capacitor regulated charge pump power supply. *IEEE, J. Solid-State Circuits*, Vol.41 (No.8): 1944-1953. ISSN 0018-9200

Ishikawa, Y. & Saito, T. (2007). Synchronization and chaos in multiple-input parallel DC-DC converters with WTA switching. *IEICE, Fundamentals*, Vol.E90-A (No.6): 1162-1169. ISSN 1745-1337

Kabe, T.; Parui, S.; Torikai, H.; Banerjee, S. & Saito, T. (2007). Analysis of current mode controlled DC-DC converters through piecewise linear models. *IEICE, Fundamentals*, Vol.E90-A (No.2): 448-456. ISSN 1745-1337

Min, K. & Ahn, J. (2002). CMOS charge pumps using cross-coupled charge transfer switches with improved voltage pumping gain and low gate-oxide stress for low-voltage memory circuits. *IEICE, Electronics*, Vol.E85-C (No.1): 225-229. ISSN 1745-1353

Myono, T.; Uemoto, A.; Kawai, S.; Nishibe, E.; Kikuchi, S.; Iijima, T. & Kobayashi,H. (2001). High-efficiency charge-pump circuits with large current output for mobile equipment applications. *IEICE, Electronics*, Vol.E84-C (No.10): 1602-1611. ISSN 1745-1353

Pan, J.; Inoue, Y. & Liang, Z. (2007) An energy management circuit for self-powered ubiquitous sensor modules using vibration-based energy, *IEICE, Fundamentals*, Vol.E90-A (No.10): 2116-2123. ISSN 1745-1337

Park, S.J.; Kang, Y.G.; Kim, J.Y.; Han, T.H.; Jun, Y.H.; Lee, C. & Kong, B.S. (2009). CMOS cross-coupled charge pump with improved latch-up immunity. *IEICE Electronics EXpress*, Vol.6 (No.11): 736-742. ISSN 1349-2543

Qiu, Y.; Xu, M.; Yao, K.; Sun, J. & Lee, F.C. (2006). Multifrequency small signal model for buck and multiphase buck converters. *IEEE, Power Electronics*, Vol.21 (No.5): 1185-1192. ISSN 0885-8993

Starzyk, J.A.; Jan, T.W. & Qiu, F. (2001). A DC-DC charge pump design based on voltage doublers. *IEEE Trans. Circuit & Syst.-I*, Vol.48 (No.3): 350-359. ISSN 1057-7122

Tanzawa, T. & Tanaka, T. (1997). A dynamic analysis of the Dickson charge pump circuit. *IEEE, J. Solid-State Circuits*, Vol.32 (No.8): 1237-1240. ISSN 0018-9200

Wei, C.L.; Wu, L.Y.; Yang, H.H.; Tsai, C.H.; Liu,B.D. & Chang, S.J. (2008). A versatile step-up/step-down switched-capacitor-based DC-DC converter, *IEICE, Electronics*, Vol.E91-C (No.5): 809-812. ISSN 1745-1353

Yamada, K.; Fujii, N. & Takagi, S. (2004). Capacitance value free switched capacitor DC-DC voltage converter realizing arbitrary rational conversion ratio. *IEICE, Fundamentals*, Vol.E87-A (No.2): 344-349. ISSN 1745-1337

Yamakawa, T.; Inoue, T. & Tsuneda, A. (2008). Design and experiments of a novel low-ripple Cockcroft-Walton AC-to-DC converter for a coil-coupled passive RFID tag. *IEICE, Fundamentals*, Vol.E91-A (No.2): 513-520. ISSN 1745-1337

Clean Energy Systems and Experiences

Edited by Kei Eguchi

ISBN 978-953-307-147-3
Hard cover, 178 pages
Publisher Sciyo
Published online 05, October, 2010
Published in print edition October, 2010

This book reports the latest developments and trends in "clean energy systems and experiences". The contributors to each chapter are energy scientists and engineers with strong expertise in their respective fields. This book offers a forum for exchanging state of the art scientific information and knowledge. As a whole, the studies presented here reveal important new directions toward the realization of a sustainable society.

InTech Europe
University Campus STeP Ri
Slavka Krautzeka 83/A
51000 Rijeka, Croatia
Phone: +385 (51) 770 447
Fax: +385 (51) 686 166
www.intechopen.com

InTech China
Unit 405, Office Block, Hotel Equatorial Shanghai
No.65, Yan An Road (West), Shanghai, 200040, China
中国上海市延安西路65号上海国际贵都大饭店办公楼405单元
Phone: +86-21-62489820
Fax: +86-21-62489821